Biomass Conversion and Biorefinery
https://doi.org/10.1007/s13399-023-04141-9

ORIGINAL ARTICLE

Optimization of delignification and cellulose isolation process from Natural cotton pods and preparation of its nanofibers with choline chloride–lactic acid eutectic solvents

Hamid Soleimanzadeh[1] · Dariush Salari[1] · Ali Olad[1] · Alireza Ostadrahimi[2]

Received: 19 December 2022 / Revised: 22 March 2023 / Accepted: 24 March 2023

Abstract
Recently, eutectic solvents (ESs) green treatment of lignocellulose biomasses attracted vast attention due to their properties. Concerning the subject, this paper aims to apply choline chloride lactic acid-based ESs for delignification and cellulose isolation optimization from extractive-free natural cotton pods (EFNCPs) to achieve the highest cellulose extraction and purity and also, consumption of ES-treated cotton pods (ESTCPs) for nano-fibrillation. The structure of each step product was characterized by applying Fourier transform infrared (FTIR), X-ray diffraction (XRD), thermogravimetric (TG), derivative thermogravimetric (DTG), field emission scanning electron microscopy (Fe-SEM), and transmission electron microscopy (TEM) methods. As the FTIR diagram shows, respectively decreasing the strength around 1515 and 1740 cm^{-1} and increasing the intensity of bands at 890, 1030, and 1210–1490 cm^{-1} are attributed to lignin removal and increasing the cellulose amount during isolation. XRD analysis results show in the extraction and nano-fibrillation process the small peaks, which were related to the lignin and other impurities eliminated and the crystallinity enhanced. The TG and DTG results indicate that during the cellulose isolation process, the narrowness of peak at 200–400 °C increased which is due to the lignin removal. Also, the results of TG and DTG show that during the isolation process by ES, the structure of cellulose fibers is almost unchanged. Also, Fe-SEM and TEM images show that during the isolation process, due to the removal of the non-cellulosic layer surface, roughness increased. The result of this study can be used for cellulose isolation optimization with unique chemical and mechanical properties.

Keywords Natural cotton po ds · Delignification · Cellulose isolation · Cellulose nanofibers · Eutectic solvents

1 Introduction

Today, environmental pollution caused by plastics and other non-degradable chemical-based polymers has become a serious global concern. So, numerous studies conducted on the use of biodegradable materials in different industries such as packaging, detergents, pharmaceutical, food, and others. In this subject, natural biopolymers, by having advantages such as lower cost, more accessibility, and higher biodegradability, attracted vast attention [1–4].

Lignocellulosic material, as the central part of plant structure, can be categorized as one of the significant promising renewable resources and their complex structure, consists of three primary polymeric materials, including cellulose, hemicellulose, and lignin. Cellulose, as the significant part of the plant cell walls, comprises 33% w/w of all vegetable matter. Cellulosic materials, as leading categories of carbohydrate macro-polymers composed of beta (1–4)-glycosidic linked chains of glucose monomers, are the most essential component of lignocellulosic material. Cellulose is the most abundant biopolymer in the world,with 10^{11}–10^{12} tons per year of production by having particular characteristics like crystallinity, low solubility, and hydroxyl group's reactivity attracted vast attention [5–8].

The distributed cellulose throughout nature is usually along with hemicellulose and lignin. Lignin, as a three-dimensional aromatic polymer bonded by a series of C–O, and C–C linkages, has a vital role in giving plants their

✉ Dariush Salari
Salari@tabrizu.ac.ir

[1] Department of Applied Chemistry, Faculty of Chemistry, University of Tabriz, Tabriz, Iran

[2] Nutrition Research Center, Faculty of Nutrition and Food Science, Tabriz University of Medical Sciences, Tabriz, Iran

Published online: 04 April 2023

structural integrity. Separation of different components of biomass before processing is necessary for better and more use of biomasses [8–11].

Among different resources which were studied for cellulose isolation, industrial residuals such as bagasse, sugar beet pulp, apple and carrot pulps, and orange peel, have been the subject of numerous investigations. Globally, cotton fiber is the dominant fiber that serves as a raw material for the textile industry, contributing at least $600 billion annually to the economy and about 25 million tonnes of cotton are produced worldwide each year. The cotton production in our region reaches 60 thousand tons. In this investigation, cotton pod, due to geographical abundance and the presence of different cotton cultivation lands, was selected as proper resources for cellulose isolation. The amount of cellulose in cotton pods is about 42% of the total dried mass, which can be used as a suitable source for cellulose separation and cellulose nanofiber preparation [12–17].

Also, various methods were investigated for cellulose isolation. Conventional separation methods require using organic solvents, a high amount of chlorinated materials, and highly acidic or alkaline solutions. Therefore, it is necessary to develop new and environmentally friendly methods to minimize the pollution caused by the use of conventional materials [16, 18–23].

Ionic liquids (ILs) have recently been considered green solvents due to their unique properties such as low vapor pressure and high thermal stability. Low vapor pressure is an essential characteristic of a solvent because it causes ease of outdoor application without worry about evaporation. Ionic liquids are formed from a combination of different anions and cations compounds whose properties such as hydrophobicity, polarity, and dissolution are adjustable [24–31].

Despite the promising properties of ILs, such as their excellent ability for the crystalline structure of cellulose degradation or removal of lignin/ hemicellulose, the disadvantages of these liquids, such as toxicity, low biodegradability, and high cost, have limited their use. On the other hand, the synthesis of most ionic liquids is not “green” and is not possible in industrial quantities [32–36].

Like as ILs, eutectic solvents (ESs), due to their unique properties, have attracted vast attention. ESs usually have low vapor pressure due to their low volatility, and low melting point and also they don’t have flammability, and toxicity, which provides the promising potential for biocatalysis, biodegradation, and treatment. Also, these types of solvents are well-known for their biocompatibility, biodegradability, and recyclability that make possible use of them more economical. Compared with ILs, ESs are easy to prepare from cheaper materials with high purities. Moreover, they have less moisture sensitivity, and this advantage makes it possible to use them in the case of wet biomass without drying and so the cost of drying significantly decreases [24, 37–41].

ESs preparation needs mild mixing of two or more solid-phase or liquid–phase or solid–liquid phase chemicals for the preparation of joint structure at 130 °C or less. These solvents prepared by hydrogen bonding comprise at least one hydrogen bond donor (HBD) such as carboxylic acids and one hydrogen bond acceptor (HBA) like quaternary ammonium salts, resulting in a clear solution with a low freezing point. It is necessary to mention as Abottt and his coworkers declared only a special ratio of HBD and HBA called deep eutectic solvents(DESs) and other prepared solvents which have similar properties to DESs but have more melting temperatures should be called ESs [32, 36, 37, 42–46].

DES has the potential to disrupt the resistive properties of biomass and hydrogen bond interactions within the chains and also crystallinity structure in mild conditions by hemicellulose and lignin removal while sugar loss due to the structure destruction is reduced. With this regard eutectic solvents (ESs) green treatment of lignocellulose biomasses attracted vast attention [47, 48].

The properties of ES had great impacts on the treatment effect and different types of ESs were prepared by mixing different kinds of HBAs and different kinds of HBDs with different molar ratios. The final properties of DES were affected by all characteristics of components in DES [49, 50].

Choline chloride–lactic acid was used as a reference in delignification trials and the results show that a high selectivity for the separation of lignin from lignocellulosic biomass and cellulose isolation which is related to the prepared ES ratio. They showed that very different solubility values were obtained for the different combinations of choline chloride and carboxylic acid. Choline chloride–lactic acid mixtures show high solubility for lignin, while cellulose was found to be immiscible with the whole series [11, 24, 49, 51].

Also, the investigation showed in the mild condition of ES treatment the temperatures and duration hours have a great impact on lignin removal and cellulose isolation (Procentese et al. 2018; Xu et al. 2016 [52].

Concerning the subject, this paper aims to apply choline chloride-lactic acid-based ESs for delignification and cellulose isolation optimization from extractive-free natural cotton pods (EFNCPs) to achieve the highest delignification and cellulose isolation and purity and consumption of ES-treated cotton pods (ESTCPs) for nano-fibrillation.

To optimize the lignin removal and cellulose extraction, modeling of influencing parameters is required. Different methods such as central composite design, Box-Behnken, Mixture Design, and Taguchi can be applied for experimental design and optimization of process or production [53–56].

The Response Surface Method (RSM) as a well-known method, is applied in experimental design, model building,

and optimization. RSM as a multivariate method, which is the combination of statistical and mathematical techniques, can help analyze problems, where a relationship between the response and the independent parameters through a response function exists. Influencing parameters on cellulose extraction have complex interactions with each other, and due to this fact, data interpretation unless with the application of the suitable method is so difficult [23, 54].

In this research in the novel experimental and mathematical investigation, choline chloride-lactic acid-based ESs with different molar ratios were prepared and used for biomass treatment at different temperatures and times for the delignification and cellulose isolation from extractive free natural cotton pods (EFNCPs) in a mild condition. The delignification and cellulose isolation amount was studied as a response to the treatment process. The cellulose-enriched biomass at the optimum condition was applied for the post-treatment process and pure cellulose isolation. For this purpose, choline chloride lactic acid pretreated biomass was used for high purity cellulosic structure achievement by using biocompatible materials with less impact on the thermal and mechanical resistance. Prepared chemically purified celluloses (CPC) was applied for nano-fibrilization by ESs which has less influence on the mechanical and thermal strength of prepared cellulose nano fibers (CNFs). Totally, the viewpoint of this research was achieving the best cellulose isolation and nano-fibrilization alongside with special mechanical and chemical properties by using green- less environmental impact method.

2 Experimental, modeling, and optimization

2.1 Experimental

2.1.1 Material

Natural cotton pods (NCPs) were prepared from Moghan agro-industrial zone. Ethanol (98% v/v), toluene (98% v/v), acetic acid (98% v/v), H_2O_2 (35%v/v), and sodium hydroxide (98% w/w), all in the analytical grade obtained from Dr. Mojallali chemical company. The other materials, including choline chloride (98%w/w), lactic acid (98%v/v), peracetic acid (40% v/v), and sodium chlorite (98%w/w) purchased from Sigma-Aldrich company. Deionized water was used in all experiments.

2.1.2 Sample preparations

To prepare NCPs powder as a by-product for the isolation process, the sample was powdered with the aid of a laboratory grinder into fine particles and sieved properly through 150 µm screen size meshes. The prepared powder oven dried for 72 h at 50 °C and was used for the extractive-free biomass preparation (after this time the moisture first content of 5% reached 0.1%).

2.1.3 Extractive-free biomass preparation

To prepare EFNCPs for the extraction process, firstly, they were milled into fine particles and extracted in the Soxhlet extraction system, according to the ASTM D-1105–96 (American Society for Testing and Materials) standard. The extraction process was conducted in three steps and each step respectively with 50 ml of ethanol-toluene (1:2) solution, ethanol, and water as a solvent with 3 g of the sample placed in the thimble filter of the Soxhlet apparatus and incubated for 4 h.

The sample after each step was transferred to a Büchner funnel for filtration and the excess solvent was eliminated. After the last step, the filtrated biomass was dried at 90 °C for 8 h and used for the treatment process [57, 58].

2.1.4 Proximate chemical analyses

Moisture, ash content determination Moisture content was determined by 44–40 of the AACC method (American Association for Clinical Chemistry- 1983). The ash content was measured by remaining residue determination after the combustion process at 550 °C for 16 h [23].

Determination of lignin content A modified standard assay (TAPPIT222 om-06) was used to measure the amount of acid-insoluble lignin (AIL). This procedure, as the general method, can be used to determine acid-insoluble lignin in all unbleached pulps [45].

Approximately 150 mg of the extractive-free sample and 3 ml of 72% (v/v) cold sulfuric acid (about 10 °C) were poured into a 100-ml Erlenmeyer flask. The sulfuric acid addition was slowly along with mixing with a glass rod.

The sample was placed in a water bath at a temperature of 20 ± 1 °C and allowed to disperse for 2 h. After 2 h, 84 ml of deionized water was poured into a 100-ml Erlenmeyer flask, and the suspension was autoclaved at 123 °C for 45 min. At the end of this period, the autoclaved sample rapidly cooled and filtered using No. 1 Whatman filter paper. The filtrate solution was collected, and the residual was washed twice with boiling water to eliminate soluble lignin and residual acid.

The residue in the filter was oven-dried at 105 ± 3 °C until a constant weight was recorded.

After drying in the oven and cooling in the desiccator for 30 min, the dried AIL was *weighed* and the lignin percentage was determined according to the following Eq. (1):

$$Lignin\% = \frac{W\ DL}{W\ EFS} \times 100 \quad (1)$$

W DL and W EFS were the weight of dried lignin and the extractive-free sample.

In this procedure, acid-insoluble lignin remained constant whereas the other carbohydrates hydrolyzed[23, 57].

Holocellulose preparation and determination Measurement of holocellulose amount (total cellulose and hemicellulose) was conducted by the Waise method with some modifications [23, 51, 57].

Holocellulose was separated from extractive-free biomass by the delignification process with sodium chlorite usage. For this purpose, approximately 500 mg of the EFNCPs was dispersed in 30 ml of 6 mg/ml sodium chlorite solution containing 0.04 mL of 10% v/v peracetic acid (pH 3.5).

The prepared mixture was incubated in the 85 °C water bath for 30 min. After this time, 200 mg of sodium chlorite powder and 0.04 mL of peracetic acid solution were added and this process was repeated seven times.

The sample was filtered through a No. 1 Whatman filter paper and washed 3 times with 50 ml of hot deionized water. The filtrate was discarded, and the residual dried at 105 ± 3 °C for 2 h.

The holocellulose percentage calculation is presented in the following Eq. (2):

$$\text{Holocellulose}\% = \frac{W\ DHC}{W\ EFS} \times 100 \quad (2)$$

W DHC and W PS were the weight of dried holocellulose and the extractive free samples respectively.

Determination of cellulose and hemicellulose Cellulose content determination was done based on the KS M 7044 (Korean Standards Association method for alpha, beta, and gamma cellulose measurement (. In this way, approximately 300 mg of prepared holocellulose was poured into a 50 ml Erlenmeyer flask and 3 mL of 17.5% w/v sodium hydroxide was added to it and mashed with a glass rod for 5 min and incubated in a 20 °C water bath for 20 min. In the next step, 3 mL of distilled water was added, and the sample and mixed well. The resulting sample was filtrated through No. 1 Whatman filter paper and washed 3 times with deionized water. Subsequently, 2.4 mL of 10% v/v acetic acid was applied for naturalization. In the last step, the sample again was washed with hot deionized water and oven-dried at 100 °C until a constant weight was reached. The final weight is considered as cellulose weight according to Eq. (3) [57].

$$\text{Cellulose}\% = \frac{W\ DC}{W\ DHC} \times 100 \quad (3)$$

W DC and W DHC are the weight of dried cellulose and dried holocellulose samples.

2.2 Preparation of eutectic solution

For this purpose, the proper molar ratio of choline chloride and lactic acid carboxylic acid (respectively as acceptors and donors of hydrogen bonds molar ratios: 1:3,1:5,1:7,1:9, 1:11) were mixed in the incubator shaker at 60 °C until achieving a clear solution. The prepared solution due to dehydration of ammonium salts absorbs moisture and therefore, after preparation should be dried (60 °C for 12 h) and stored in closed containers [23, 32].

2.2.1 Investigation of lignin removal and cellulose separation by ES solvents

Eutectic solvents have a limited ability to dissolve the lignin and separate cellulose. To investigate the degree of dissolution, different molar ratios of lactic acid–choline chloride ES were prepared.

Next, to investigate the lignin removal, the appropriate weight ratio of EFNCPs completely dried powder and predried ES (1:20 w/w) mixed together. The delignification process was investigated at different temperatures and times along with stirring in the oil bath.

After pretreatment with the ES at different temperatures and times, the same initial volume of boiling deionized water and ethanol solution was added and the separation process was performed for 30 min. This process was repeated two more times with boiling deionized water. The pretreated sample was put into a vial and placed in an orbital shaker incubator and mixed at 200 RPM at 50 °C for 20 min. The water was decanted and the water-washing process was repeated 3 times to ensure that the ES was removed totally (the product of this step is called ES-treated cotton pods (ESTCPs) powder).

Finally, the sample was drained with a 20-µm nylon filter and dried at 60 ± 2 °C oven for 12 h. The refined sample was used to measure lignin, hemicellulose, and cellulose in the structure.

As mentioned, ES has a limited ability to dissolve the lignin and separate soluble, and therefore the post-treatment process is necessary. This research aims to develope a green method for cellulose isolation, using biocompatible materials such as acetic acid, peracitic acid, water, and hydrogen peroxides with low concentration. After this treatment, cellulose remains with high purity [24].

In this stage, unlike the previous stage, due to the opening of the lignocellulose network, the time and conditions of treatment are much milder and there was no need to use a high concentration of materials. The post-treatment was

done by the addition of 1 g of pretreated sample to 10 ml of H_2O_2 6% v/v which the pH of that was pre-adjusted at 3 by acetic acid. For this purpose, the mixture was completely stirred about 10 min at room temperature (this process was done for remaining lignin elimination). The treated sample at the last step was treated with 10 ml of 6% w/v NaOH solution containing 3% v/v H_2O_2 (to remain hemicellulose removal). The sample was washed three times by boiling deionized water and filtrated with No.1 Whatman paper and used for the last analyses and structure determination. The resulting material is called chemically purified cellulose (CPC).

2.2.2 Preparation of cellulose nanofibers

CPC has been used for cellulose nanofibers (CNFs) production with ES solvent. In this step, about 2 g of completely dried extracted CPC was treated with 30 ml of previously prepared and dried ES (with the 1:10 molar ratio of choline chloride-lactic acid, dried at 80 °C) for 30 min.

To complete ES removal, approximately 100 ml of hot deionized water was poured into the mixture and centrifuged at 4000 rpm and the solvent was eliminated. The process of washing was repeated 3 times. The prepared CNF dispersed well by ultra turrax homogenizer (t-25-IKA) and was freeze-dried at − 85 °C for 2 h and used for complementary investigations.

2.2.3 Cellulose characterization

Functional groups of EFNCPs, ESTCPs, CPC, and CNF were identified by Fourier transform infrared (FT-IR) spectra (The Tensor 27 spectrometers-Bruker, Germany).

In the sample preparation step, 2 mg of each sample was mixed with 200 mg of potassium bromide (KBr) and transmittance data (%) were recorded from 500 to 4000 cm^{-1}.

Cellulose crystallization determination was done based on X-ray diffraction (XRD) method results. The XRD pattern data was collected on a SIEMENS D500 diffractometer (Germany) and Cu Kα radiation (λ = 1.54 Å) from 10 to 80° 2θ with the 0.25° step size per minute.

The cellulose Crystallinity Index (CrI) was calculated using the following Eq. (4):

$$\mathrm{CrI}\% = \frac{\mathrm{A\ cr}}{\mathrm{A\ sample}} \times 100 \tag{4}$$

A in the presented equation is the area under the sample intensity curve associated with the total crystalline phase (for all calculations the background should be eliminated).

Thermogravimetric (TG) analysis and derivative thermogravimetric (DTG) analysis were performed in Mettler Toledo instrument. The experimental setup consisted of a 10°C/min linear heating program from 30 to 600 °C, with 30 mL/min N_2 low rates.

Field emission scanning electron microscopy (FE-SEM) (MIRA3 FEG-SEM, Czechia) and transmission electron microscopy (TEM) (LEO 906 E- Germany) microscope at an acceleration voltage of 120 kV were applied for surface morphology investigation of NCP, ESPC, CPC, and CNFs.

2.3 Computational details

Optimizing cellulose extraction conditions for achieving the maximum extraction amount is aimed to be done by application of the Response Surface Methodology-Central Composite Design (RSM-CCD) system. To develop an experimental database RSM method is applied and experimental results are used to achieve optimum isolation conditions.

2.3.1 DOE and statistical analysis

There are several ways to experimental design. The design of the experiment (DOE) method, as a strong tool was used for factor optimization in different processes and products to achieve the best condition. The RSM-CCD as a suitable design method can be used for polynomial modeling establishment and involved parameter efficiency determination to reach optimal conditions[23, 54].

A Central composite design (CCD) method with $\alpha = \pm 2$ (to avoid decimal values and make easy control of preparation and process parameters) was used for studying the effect of three main parameters on cellulose isolation and delignification yield. The Software of Design Expert (8.0.7.1 version) was applied for experimental design. Three main parameters which have been selected for this purpose are the process temperature (°C), ES solvents ratios (mol acceptor: mol donor), and process time (h). The lower and upper levels and center points of these parameters were selected according to the previous studies[24, 52, 59].

Table 1 represents the actual and coded values of independent variables. The following Eq. (5) was used for encoding actual parameters:

$$X_i = \frac{X_i - X*_i}{\Delta X_i} \tag{5}$$

X_i and x_i respectively show the coded and uncoded value of the i'th parameter. x_i^* is the x_i regarding value at the Central point in the studied area, and Δx_i is the step size [54].

Due to the possibility of interaction between parameters the linear and zero-order models cannot correlate response and input variables correctly and have more lack of fit and also lower R^2 values and so a second-order polynomial equation was used for correlation between response and involving parameters. The modeling was carried out by adjusting

Table 1 The levels of the independent operation variables in actual and coded value [24, 52, 59]

Variables		Ranges and levels				
		-2	-1	0	+1	+2
Choline chloride/ lactic acid / molar ratio	X1	1:3	1:5	1:7	1:9	1:11
Process temp (°C)	X2	80	90	100	110	120
Time h	X3	1	2	3	4	5

the second-order polynomial equation to the experimental results of the response. Analysis of variance (ANOVA) was performed to confirm the adequacy of the predicted model by assessing the lack of fit, regression coefficient (R^2), and the p and F-values obtained from Analysis of variance (ANOVA). The validated model can be plotted in form of 2 and 3-D graphs to generate surface response for the determination of the best operation conditions.

The R^2 value near unity shows the fitness quality of the model. The p values of parameters and models lower than 0.05 show the model terms are significant. Also, the p-value of more than 0.05 for lack of fit shows the model's ability to contribute to response and influencing parameters.

The response assessment process can be done by. The perturbation, and 2-dimensional (2D) contour plots based on the established model can clarify the effect of each parameter and the interaction between them. While flat lines in the perturbation plot indicate that the response is not sensitive to the change of a factor, a steep slope or curvature shape shows sensitivity to that [54].

To evaluate the differences between all parameters at a particular point (e.g., Central point) in the design space, the perturbation plots were applied. A steep slope or curvature form in a parameter shows response sensitivity to that. When the lines are relatively flat represent that response is not sensitive to change in specific factor [54].

Contour plots represent the relationship between the independent and dependent variables. These plots show the correlation between two variables on delignification and cellulose amount when the third parameter is kept constant. While the elliptical or saddle shape of contour plots represents the interaction considerability, the plot's circular mode displays that the interaction between parameters can be neglected [54].

To obtain the optimum conditions for achieving the highest delignification and cellulose in the structure, the optimization tool of Design Expert software has been applied. This procedure has been done for maximization of delignification and cellulose isolation. Numerical optimization uses the models to search the factor space for the best trade-offs to achieve multiple goals. A verification experiment should be conducted under the predicted conditions and empirical responses that were close to the estimated amount shows the validity and adequacy of the obtained models.

3 Results and discussion

In this work, the effect of different choline chloride lactic acid ES pretreatment conditions on the efficiency of NCP delignification and cellulose isolation was investigated and optimized using the RSM-CCD method. The treated sample at the optimum condition was used for more process and cellulose Nano-fiber preparation.

Having an outlook of the initial structure and composition of NCP is necessary. For this purpose, chemical determinations of the main material in the NCP structure are processed according to declared methods. The experimental results of moisture, ash, lignin, hemicellulose, and cellulose determination in NCP are presented in Table 2.

3.1 Mathematical results and modeling

3.1.1 RSM-CCD and ANOVA results

EFNCP with different amounts of lignin and cellulose in structure was investigated as raw material for delignification and cellulose isolation process with choline chloride ES at the different conditions of temperature and time according to the experimental design. The matrix regarding experimental design conditions by the RSM-CCD method and corresponding lignin, holocellulose, and cellulose amounts is shown in Table 3.

The following second-order polynomial equations model the lignin and cellulose amount (Y1: lignin percentage, Y2: cellulose percentage) regarding the influencing

Table 2 Percent of different materials in extractive-free natural cotton pods

Chemical	Percentage w/w%
Cellulose	27.50 ± 0.20
Lignin	40.00 ± 0.20
Hemicellulose	21.50 ± 0.21
Ash	3.00 ± 0.05
Other extractive materials	3.00 ± 0.05
Moisture	5.00 ± 0.05

Table 3 Design matrix and correlated values

Run Order	Uncoded Values			Amount of cellulose, hemicellulose, and lignin material in primary treated (treatment with ES)		
	Choline Chloride: lactic acid molar ratio	Process Temp (°C)	Time (h)	Lignin%	Holocellulose%	Cellulose%
1	1: 11	100	3	26.8391	63.1505	44.7446
2	1: 7	100	3	29.9048	62.9913	42.919
3	1:3	100	3	29.8905	60.2057	40.1844
4	1:7	120	3	24.664	67.8311	46.5465
5	1:7	100	3	28.6236	62.546	42.8339
6	1:7	100	5	25.528	63.936	43.729
7	1:5	90	2	28.7966	60.4627	40.4651
8	1:5	90	4	27.8659	60.1926	40.1551
9	1: 9	90	4	27.54	63.7826	42.5888
10	1:7	100	3	28.5367	62.6988	42.1851
11	1:7	80	3	27.6164	62.9319	39.6774
12	1:5	110	4	29.1364	61.4836	41.0617
13	1:7	100	3	29.312	61.982	42.007
14	1:9	110	2	27.3019	61.1399	44.2339
15	1:9	110	4	22.5456	68.1812	48.7088
16	1:7	100	3	28.85	62.3503	41.8581
17	1:9	90	2	31.0345	59.2346	40.0508
18	1:7	100	1	30.0198	60.1437	41.0795
19	1:5	110	2	28.9377	62.5271	41.5159
20	1:7	100	3	28.5784	61.6498	41.9968

parameters variation (the values are coded- insignificant terms were eliminated).

$$Y1 = -0.6686X2^2 - 0.2602X3^2 - 1.27X1X2 - 0.9398X1X3 - 0.7761X1 - 0.8263X2 - 1.12X3 + 25.82 \quad (6)$$

$$Y2 = +1.04X1X2 + 0.9721X1X3 + +1.34X1 + 1.62X2 + 0.7217X3 + 42.43 \quad (7)$$

In these equations as mentioned in Table 1., X1 and X2, and X3 are respectively choline chloride: lactic acid molar ratio, process temperature, and process time in coded values. The coefficient of X1, X2, and X3 show a variable direct effect on the response. As well as a direct effect of parameters on the response they can interact with each other and strengthen the parameter's effect on the response which can be shown by X1X2, X1X3, and X2X3 coefficients. In the coded equation the coefficient of each variable shows the importance of that parameter on the response as the dependent variable.

Established models variance analyses in presented in Table 4. As the R^2 results show the presented models have a good ability to correlate the response and involving parameters (Fig. 1). The *p*-values lower than 0.0001 for both models (less than 0.05) and a high amount of *F*-values (43.81and 67.95 for lignin and cellulose percentage) show this fact. Also, the lack of fit *p*-values which were 0.6923 and 0.3349 respectively, validate these sentences.

The adequate precision for lignin and cellulose amount in the structure were 26.9431 and 30.7995 which are more than 4 (signal-to-noise ratio) show that models can navigate the design space.

The coefficient of variation (CV) of less than 10%, shows the model's reproducibility. The CV value of 1.74% and 1.25% for lignin and cellulose amounts demonstrate good precision of experiments.

3.1.2 Variable effect on perturbation, response surface, and counter plots

The perturbation plot regarding the lignin and cellulose percentage in the ESTCPs is presented in Fig. 2. As this figure shows all three influencing factors, including lactic acid: choline chloride ratio, process time, and temperature have direct effects on lignin elimination and cellulose isolation percentage in the pretreated sample, so that by lignin amount decreases in the structure cellulose amount increase.

As previously mentioned, by using contour plots the relationship between different parameters (including lactic

Table 4 ANOVA for cellulose isolation

Source of	Sum of squares Y1	Sum of squares Y2	DFbY1	DFbY2	Mean square Y1	Mean square Y2	*F*-value Y1	*F*-value Y2	*p*-value Y1	*p*-value Y2
X1	9.64	28.90	1	1	9.64	28.90	40.50	102.55	< 0.0001	< 0.0001
X2	10.92	42.24	1	1	10.92	42.24	45.90	149.89	< 0.0001	< 0.0001
X3	21.17	8.33	1	1	20.17	8.33	84.78	29.57	< 0.0001	< 0.0001
X1X2	12.85	8.70	1	1	12.85	8.70	53.99	30.89	< 0.0001	< 0.0001
X1X3	7.07	7.56	1	1	7.07	7.56	29.69	26.82	0.0001	0.0001
$X2^2$	11.78		1		11.78	-	49.51	-	< 0.0001	-
$X3^2$	1.78		1		1.78	-	7.50	-	0.0180	-
Model	72.98	95.75	7	5	10.43	67.95	43.81	67.95	< 0.0001	< 0.0001
Residuals	2.86	3.95	12	14	0.2380	0.2818				
Lack of fit	1.39	2.89	7	9	0.1985	0.3213	0.6768	1.52	0.6923	0.3349
Pure Error	1.47	1.05	5	5	0.2933	0.2109				
Total	75.84	99.70	19	19						
Y1: $R^2 = 0.9623$, Adequate precision = 26.9431, CV = 1.74%										
Y2: $R2 = 0.9604$, Adequate precision = 30.7995, CV = 1.25%										

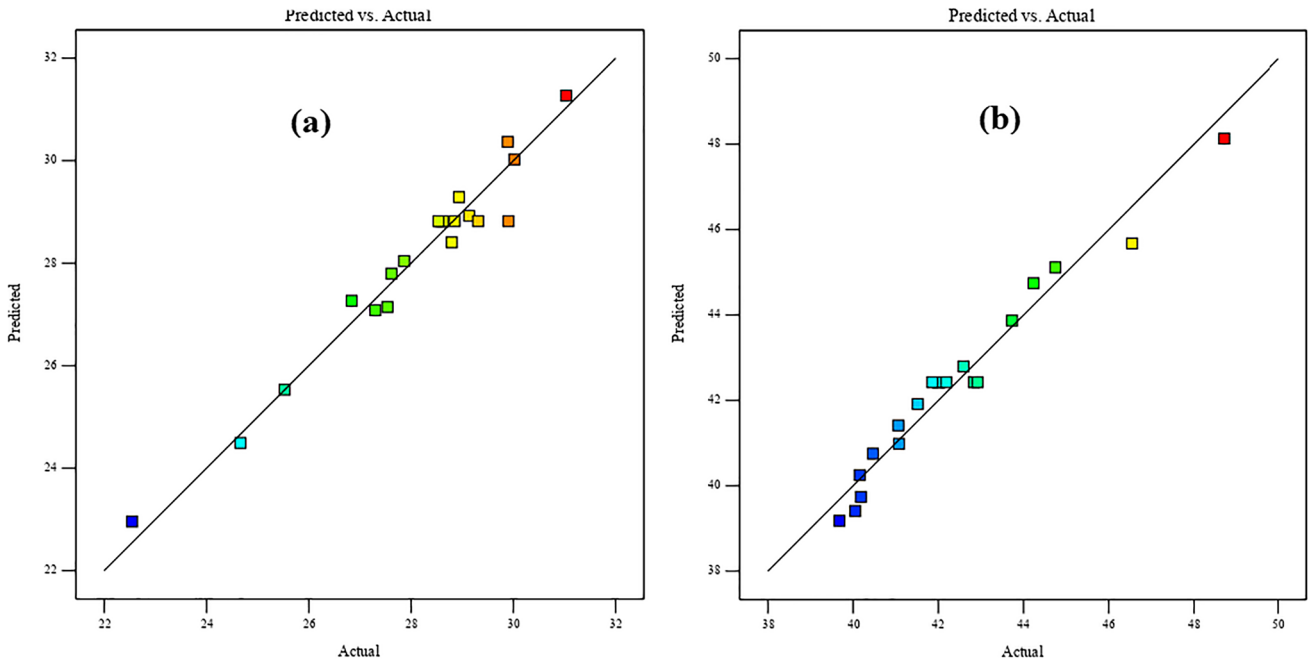

Fig. 1 Predicted versus actual plot for **a**) lignin percentage and **b**) cellulose percentage in the structure after treatment with ESs

acid: choline chloride ratio, process time, and temperature) on lignin and cellulose percentage after treatment with ES can be illustrated (as shown in Fig. 3). Figure 3a and 3c respectively demonstrates the contour plots of lignin and cellulose percentage regarding the different amounts of ES ratios and temperature at the constant time (3 h). According to the saddle shapes of the contour plots, there is effective interaction between temperature and ES ratio. It is clear from the figure that the lignin and cellulose percentage amount respectively decreases and increases by increasing the ES ratio or temperature. The lowest lignin percentage and highest cellulose amount in the structure are achieved when the amount of ES ratio is about 7 to 11 and the process temperature is between the 901–20 °C.

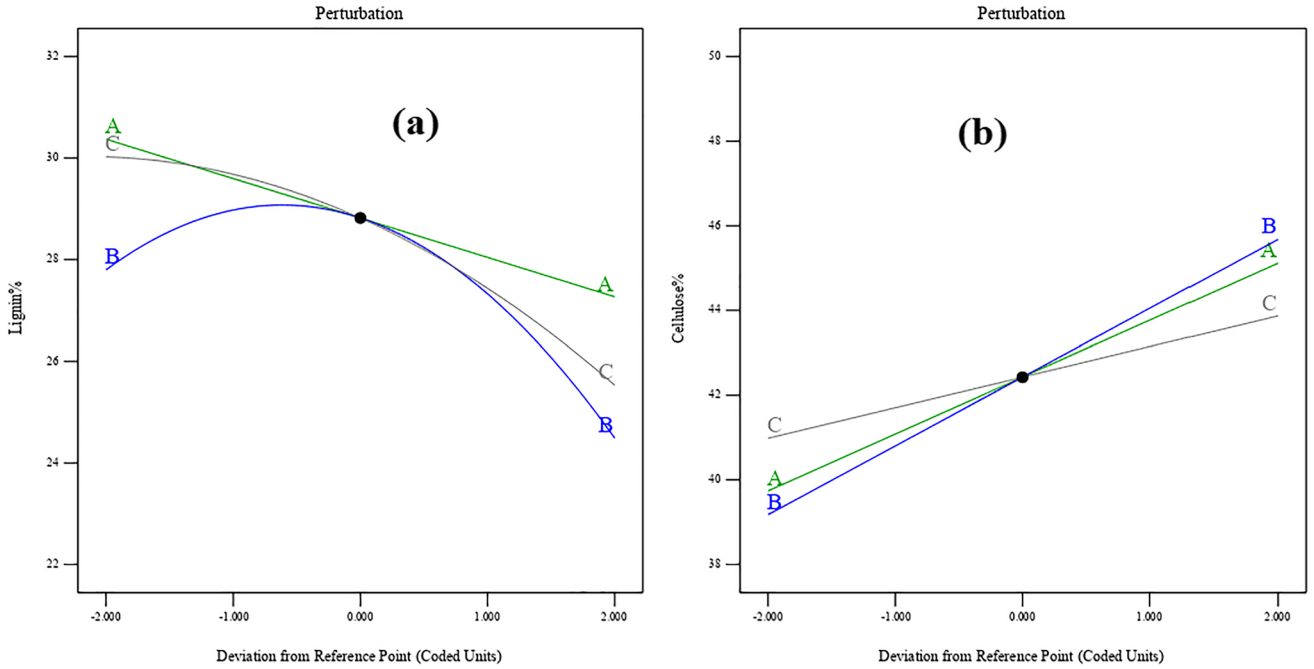

Fig. 2 The perturbation plot regarding the **a**) lignin percentage **b**) cellulose percentage in the structure after treatment with ES solvents (A: choline chloride: lactic acid molar ratio, B: process temp (°C), C: time (h))

It was suggested that by increasing the choline chloride lactic acid molar ratio and temperature increase the viscosity decreased and the ability of ES for delignification enhances. It should be mentioned higher temperatures cause ES destruction and decrease its ability in the process. Also, it was reported in the more than 1:12 choline chloride lactic acid ratio the acidic property of ES solvent is dominant and can change the structure. For this purpose, most of the investigation has been conducted in the range of 1:1 to 1:12 [24, 52, 60, 61].

Figure 3b and d shows the lignin and cellulose percentage as a function of the ES ratio and the processing time at the constant temperature (100 °C). According to the contour plot's saddle shapes, the interaction between variables is significant. As it can be understood from this figure, the delignification and cellulose isolation percentage increases by ES ratio or process time values. The most delignification and cellulose isolation percentages were achieved when the ES ratio and the temperature were at. 7–11 ratio and 3–5 h. This result was validated by other investigations that by increasing the time of treatment the delignification amount increases [61].

It should be mentioned the lignin amount in the structure is consistent with cellulose percentage (as the lignin amount during treatment by ES in the structure decreases cellulose percentage increases which are due to the high ability of ES in lignin solubilization) [62].

3.1.3 Optimization and validation of responses

To achieve the maximum delignification and obtain the most cellulose extraction amount, the Design Expert software optimization tool was applied. This procedure is used for lignin removal and cellulose isolation maximization (between zero and one). The optimization condition by desirability method and best conditions for pretreatment are represented in Table 5. Under predicted conditions, the verification experiment was repeated and experimental responses were close to the estimated amount.

The optimum condition which suggested by the design expert numerical optimization tool applied for the post-treatment process. The amount of lignin and cellulose in different samples is presented in Fig. 4.

3.2 Experimental results and characterization

3.2.1 FTIR analysis

Typical FT-IR spectra related to the functional group of EFNCPs, ESTCPs, CPC, and CNF are presented in Fig. 5.

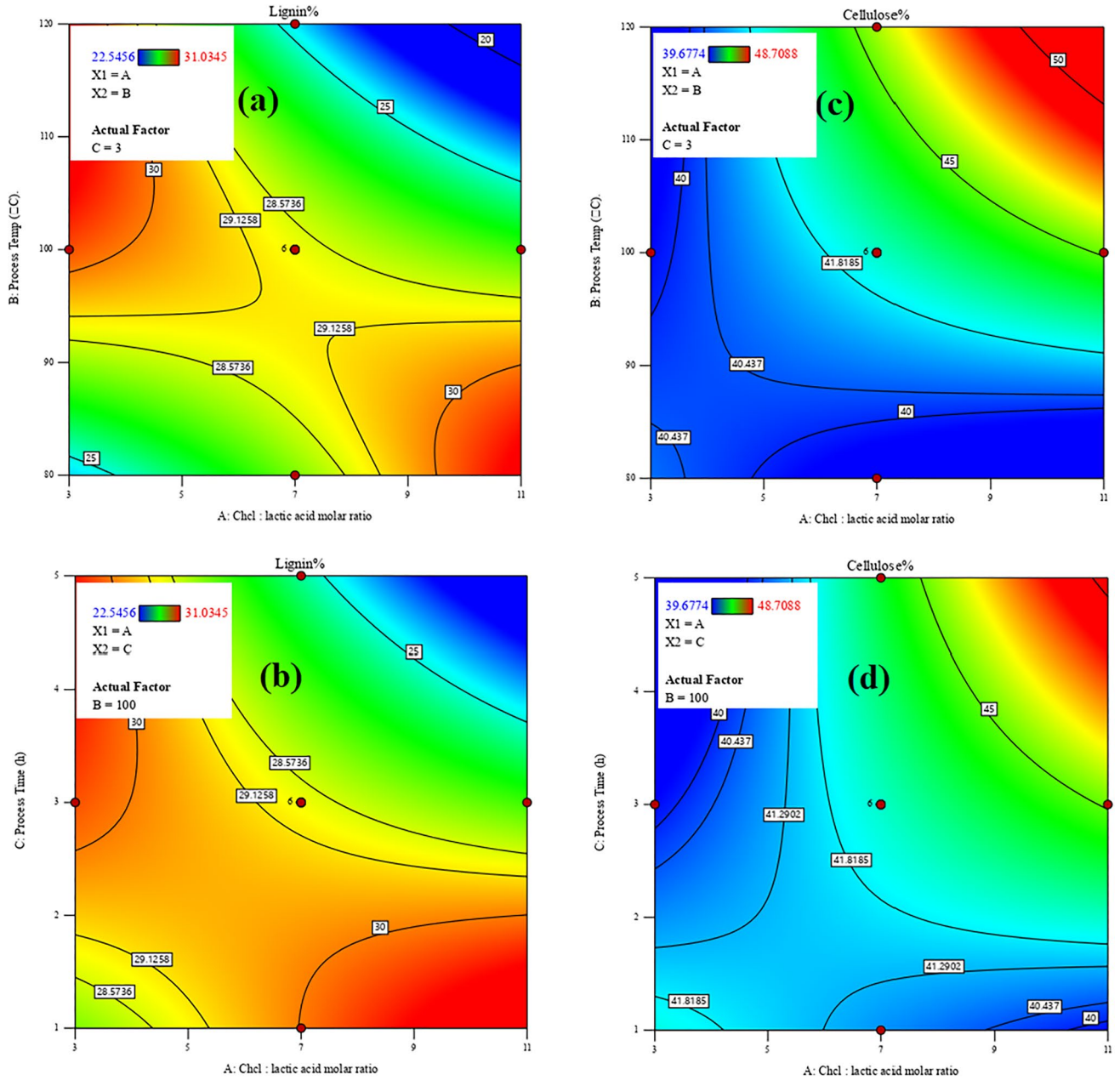

Fig. 3 Contour plot image of the effect of different parameters on lignin and cellulose percentage after treatment with ESs

This figure shows that all spectra have similarities that are related to the base's similar chemical compositions.

As it is clear in a structure of NCP, EPC, and CPC a broad absorption band at 3400–3500 cm^{-1} related to the tensile vibrations of -OH groups in the cellulose structure is observed. Also, it was mentioned there is a negligible effect on hydrogen bonding in the cellulose after ES treatment [63–65].

Regarding the obtained results, in a structure of EFNCP, ESTCPs, CPC, and CNF in a range of 2860 cm^{-1}, and 2940 cm^{-1}, an absorption peak was observed, which shows tensile vibrations aliphatic saturated C-H associated with methylene groups in the structure of the desired materials [62, 66].

In the spectrum of EFNCP, an absorption peak around 1740 cm^{-1} is related to the C = O group vibration in the acetyl or ureic ester group of hemicellulose or steric bonds in the lignin structure. In the process of ES treatment and after the cellulose complete isolation process in the ESTCP, CPC, and CNF structures, this peak strength decreased and was eliminated which shows the lignin and hemicellulose removal. Also, the FTIR vibration at near 1515 cm^{-1}

Table 5 Optimization condition and optimum values of ES treatment for achieving maximum delignification and cellulose isolation

Optimization condition							
Parameter			Lower	Upper	Goal	Importance weight	
Choline chloride lactic acid ratio		is in range	3	11			
Process Temp (°C)		is in range	80	120			
Process Time (h)		is in range	1	5			
Lignin%		minimize	22.5456	31.0345	minimize	1	
Cellulose%		maximize	39.6774	48.7088	maximize	1	
Optimum values							
Parameter	Choline chloride lactic acid ratio	Temperature	Time	Predicted cellulose isolation amount%	Experimental cellulose amount%	Predicted lignin amount%	Experimental lignin amount%
amount	1:10.01	118 °C	4.56 h	53.66	54.12	15.89	16.05

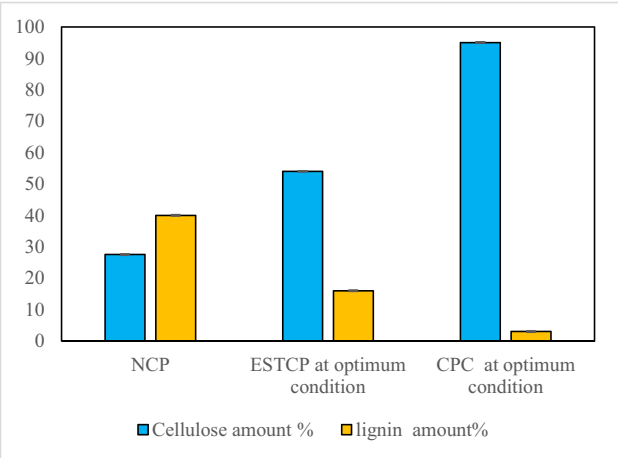

Fig. 4 The amount of lignin and cellulose in different samples with the standard deviation ± 0.2

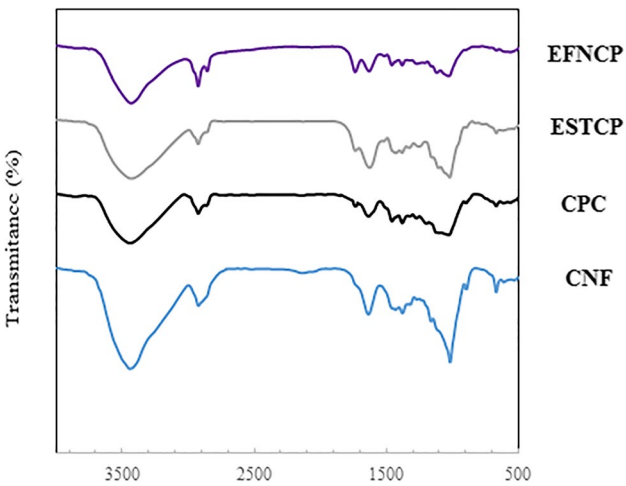

Fig. 5 FTIR Analysis of different forms

indicates the lignin aromatic ring skeletal stretch. As it is clear during the ES treatment and isolation process the intensity of this peak decrees [67–70].

In the FTIR spectrum of EFNCP, ESTCP, and CPC, an absorption peak around 1630 cm^{-1} was observed which is related to the hydroxyl group vibration and water absorption [71].

Several peaks were observed in the EFNCP, ESTCP, CPC, and CNF structures in the 1210–1490 cm^{-1} and 1055 cm^{-1} regions. These are associated with symmetric and asymmetric vibrations of carboxylic acids, CH, and CO in the cellulose and hemicellulose structure [72]. Also, the peak around 1030 cm^{-1} is related to the vibration of C–O–C in the pyranose ring in the cellulose structure. More intense vibrations at these regions show increasing the cellulose amount during the treatment and isolation process [62]. Also, the increase of band at 890 cm^{-1} in the ESTCP, CPC, and CNF in comparison to EFNCPs is related to the glycosidic linkages of the glucose ring of cellulose in the cellulose typical structure which shows increasing the amount of cellulose in the structure along the isolation process [73].

Absorption peaks indicating the bending vibrations of C–OH groups in the structure have been reported for EFNCP, ESTCP, and CPC structures in the 650 cm^{-1} region. As reported in some literature, the strength of this peak is related to prepared cellulose nanostructures [74, 75].

3.3 XRD analysis

The XRD pattern of EFNCP, ESTCP, CPC, and CNF samples is demonstrated in Fig. 6. With regards to the existing results, the primary peaks appear at about 16° and 22.5° respectively, which shows the cellulose phase in the structure.

As it is clear, the XRD result shows that the EFNCP has different impurities that are obvious in the XRD patterns

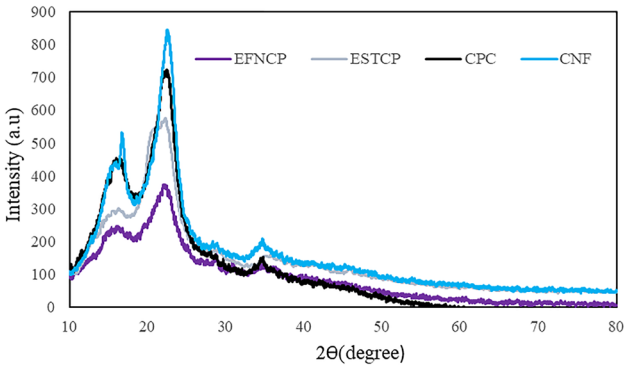

Fig. 6 XRD Analysis of EFNCP, ESTCP, CPC, and CNF

Table 6 Crystallinity Index

Sample	CrI %
EFNCP	23.30%
ESTCP	42.01%
CPC	46.13%
CNF	53.50%

by small peaks. In the exaction and nano-fibrillation process, the small peaks were eliminated, and the crystallinity increased [76, 77].

As it is clear from this figure the diffraction patterns of all materials showed characteristic peaks of cellulose at the same range which shows that the crystal morphology of cellulose did not change during the treatment but that the crystallinity was increased during the separation and nano-fabrication processes [78].

The cellulose Crystallinity Index (CrI) was calculated using the 4 equation and the CrI results are reported in Table 6. It is obvious from these results in the extraction process by structure cleavage and impurities like lignin elimination the fibrillation increases and crystallinity enhances [22].

3.3.1 TG and DTG analysis

Figure 7a indicates the TG curves of EFNCP, ESTCP, CPC, and CNF. All TG curves show a small preliminary drop between 50 and 150 °C, which corresponds to a mass loss of about 5% of absorbed moisture. The decomposition of the original untreated plant fibers occurs in several stages, indicating the presence of different components that decompose at different temperatures. Due to the low decomposition temperature of hemicelluloses and lignin, EFNCPs begin to degrade from about 200 °C, and the glycosidic bonds of cellulose are broken. A small shoulder appeared in the EFNCP DTG curve at 250 °C, which corresponds to the hemicellulose decomposition, which is removed during the isolation process. The peaks on the DTG curve (Fig. 7b) correspond to the temperature of the maximum decomposition rate. The wide peak in the 200–400 °C region is related to cellulose degradation. As mentioned in previous articles, the peaks in EFNCPs around 450–650 °C are related to the lignin remaining in the structure. During isolation by the removal of lignin and hemicellulose, the narrowness of the peaks increased. As it is clear during isolation by ES treatment, impurity-related peaks are removed, which is consistent with FTIR and XRD analysis. Furthermore, as it is clear in the nano-fibrillation process by ES, the maximum thermal decomposition temperature of cellulose is only 12 °C lower than that of EFNCPs (and 6 °C lower than isolated CPC), which indicates the structure of cellulose fibers is almost unchanged. This suggests that the CNF prepared by this procedure is highly heat resistant and can be used for specific subjects [79–83].

3.3.2 Fe-SEM and TEM

Figure 8 represents respectively the Fe-SEM image of EFNCP, ESTCP, CPC, CNF, and TEM and the size distribution of CNFs. AS Fig. 8a shows, the surface layers have some impurities (lignin, oil, etc.) and have an undisrupted, rigid, homogenous surface. Figure 8b demonstrates the ESEPCs structure after the ESs application process and lignin removal. As it is clear in the primary treatment process with ES the surface homogeneity decreases and fiber bundles appeared which is due to the lignin elimination. Figure 8c shows the CPC fibrils after the post-treatment process, including delignification, and removal of hemicellulose and other residuals. As it is shown after the post-treatment process the cellulose fibers become clear and impurities are highly eliminated.

As can be assumed from Fig. 8b and c in the process of EFNCP pretreatment with ES and post-treatment process for lignin and hemicellulose removal, surface roughness increased. The increase in surface roughness is related to the non-cellulosic layer removal (hemicelluloses and lignin) during each treatment process. The increase in surface roughness was produced by the pretreatment process, since the hemicelluloses coat the cellulose fibrils, whereas lignin fills the empty spaces [84, 85].

The prepared CNFs structures by ES solvent treatment are demonstrated in Fig. 8d.

It can be understood that treatment and nano-fibrillation by remaining impurities and amorphous region elimination alongside structure cleavage cause cellulose fibrils' size and diameters decrease and their crystallinity and uniformity enhance.

The morphological structure of the prepared CNFs was studied by transmission electron microscope (Fig. 8e).

For transmission electron microscopy (TEM), the frieze-dried cellulose nanofibers were diluted by ultrapure deionized water and dispersed by ultra-sonication (30 min at 20 Hz). A small droplet of 0.005% (w/v) cellulose

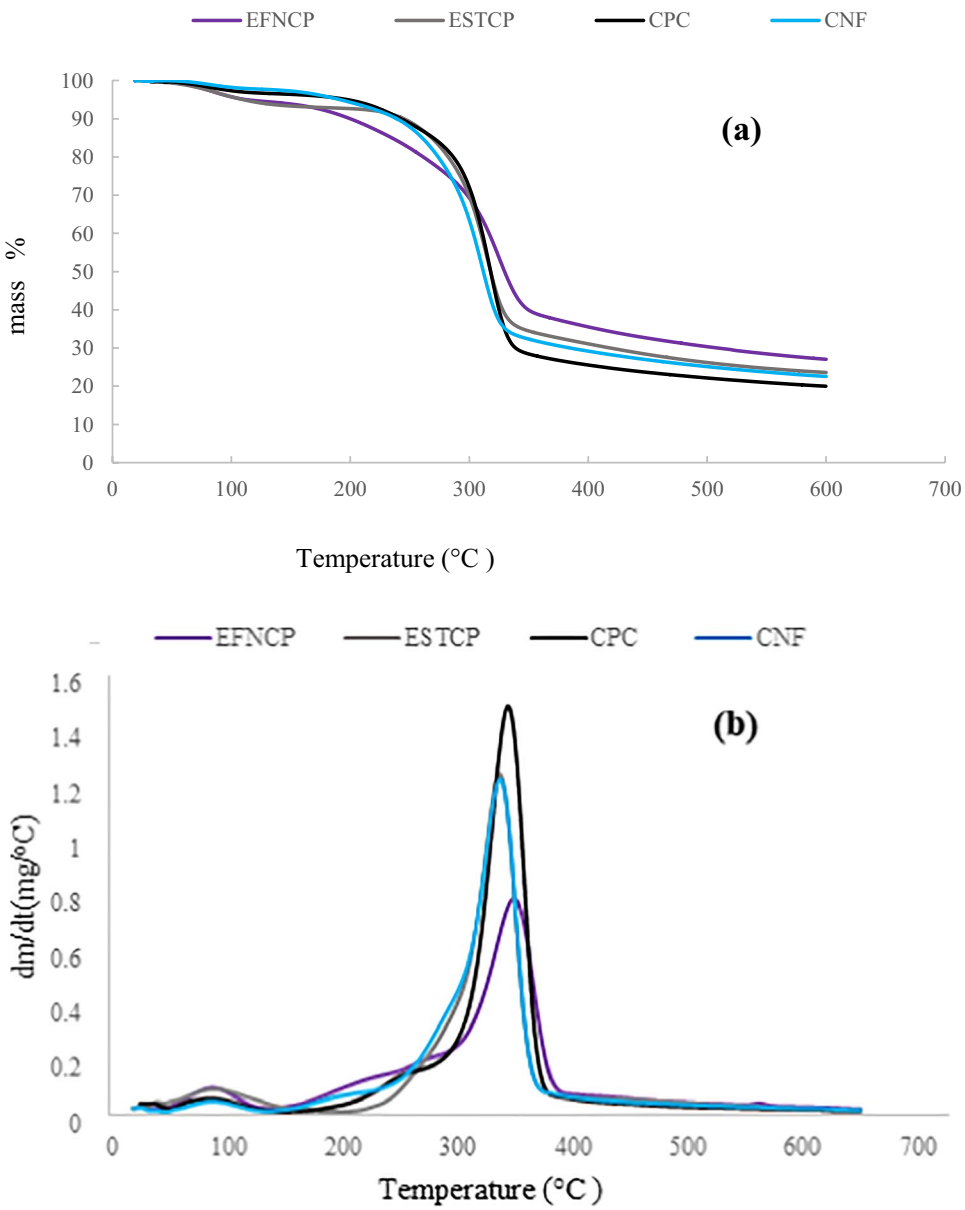

Fig. 7 **a**)TG and **b**) DTG curves of EFNCP, ESTCPs, CPC, and CNF

nanocrystal suspension was added to the carbon-coated electron microscopy grid and excess solvent was eliminated by drying at room temperature.

As TEM results show after ES treatment of CPC, the morphology and surface obviously changed. As it is shown from the TEM and size distribution histogram (Fig. 8f) the prepared CNFs with smooth surfaces have short rod shapes and high aspect ratio with diameters of 20–40 nm, and lengths of 400–800 nm. The changes in fiber size are related to the glycosidic linkage cleavage of prepared EFNCPs during the cellulose isolation and nanofibrillation process in the presence of ES solvents.

4 Conclusion

Concerning all of the subjects mentioned in this investigation, this paper aims to apply choline chloride- lactic acid-based ESs for delignification and cellulose isolation

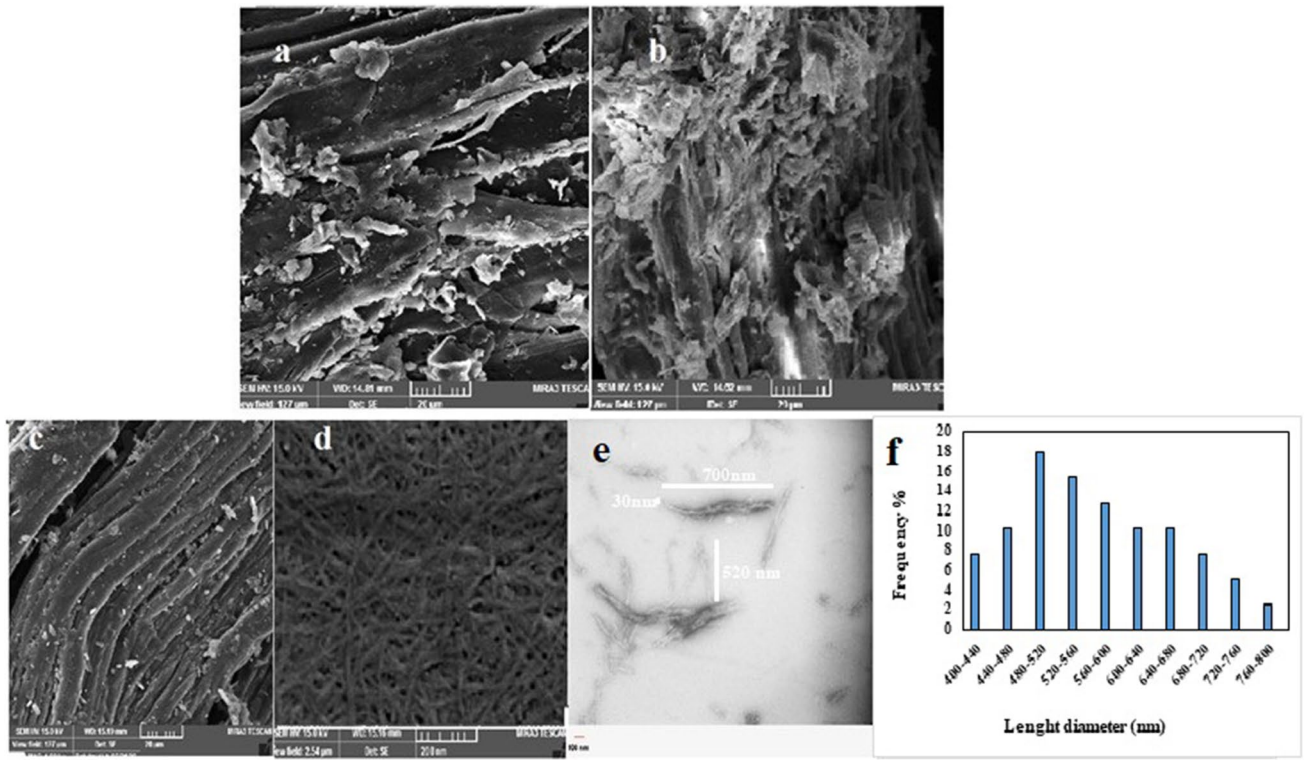

Fig. 8 Fe-SEM and TEM images of different forms (**a**: EFNCP, **b**: ESTCPs and **c**: CPC, **d**: CNF, **e**: TEM image of CNF and **f**: histogram of size distribution frequency%)

optimization from extractive-free natural cotton pods (EFNCPs) to achieve the highest cellulose extraction and purity and consumption of ES-treated cotton pods (ESTCPs) for nano-fibrillation**.** The relationships between various parameters affecting delignification and cellulose separation are illustrated using contour plots. The optimum condition for cellulose isolation reaches 1:10.01 choline chloride lactic ratio, 118 °C temperature, and 4.56 h. Under optimal conditions, the experimental separation test conducted and experimental cellulose extractions performed were close to the predicted values that validated the optimization and modeling process. The primary treated biomass at the optimum condition was secondary treated in mild conditions with H_2O_2 and NaOH solution and high purity cellulose structure with 95% pureness obtained. The extracted cellulose was used for cellulose nano-fibrillation, and choline chloride-lactic acid-based ES treatment was applied for this purpose. In the process of treatment and nono-fibrillation, all of the samples were characterized by FTIR, XRD, TG, DTG, and Fe-SEM methods. The results show in the treatment process as impurities related to the lignin and hemicellulose presence eliminate and the surface morphology becomes smoother and the crystallinity index enhances. TG analyses alongside DTG analyses show that there is little difference in the maximum thermal decomposition temperature of cellulose and source biomass. TEM and Fe-SEM analyses which show the high length-to-width ratio of prepared nanofibers is in contestant with TG analyses show the mechanical and thermal strengths of isolated nanofibers is almost unchanged which is due to the mild isolation and nano- fibrillation process. The result of this investigation can be used for cellulose isolation optimization with special chemical and mechanical properties in a green and environmentally friendly method.

Abbreviations AIL: Acid-insoluble lignin; ANOVA: Analysis of variance; CNFs: Cellulose nanofibers; CCD: Central composite design; CPC: Chemically purified cellulose; CV: Coefficient of variation; CrI: Crystallinity index; DOE: Design of the experiment; ES: Eutectic solvent; ESTCPs: Eutectic solvent-treated cotton pods; EFNCPs: Extractive free natural cotton pods; Fe-SEM: Field emission scanning electron microscopy; FTIR: Fourier transform infrared; HBA: Hydrogen bond acceptor; HBD: Hydrogen bond donor; ILs: Ionic liquids; NCPs: Natural cotton pods; RSM-CCD: Response surface-Central Composite Design; TEM: Transmission electron microscopy; TGA: Thermogravimetric analysis; DTGA: Derivative thermogravimetric analysis; XRD: X-Ray Diffraction

Author contribution H.Soleimanzadeh, D.Salari, A.Olad, and A.Ostadrahimi contributed to the design and implementation of the research, to the analysis of the results and writing of the manuscript.

Data availability All datasets are available by corresponding author agreement.

Declarations

Ethical approval Hereby, we assure you that for this manuscript, all the material are the authors' own original work that reflects research and analysis results in a truthful and complete manner. This manuscript has not been previously published elsewhere and also, is not currently being considered for publication elsewhere.

Competing interests The authors declare no competing interests.

References

1. Zhao D, Zhu Y, Cheng W, Chen W, Wu Y, Yu H (2021) Cellulose-based flexible functional materials for emerging intelligent electronics. Adv Mater 33(28):2000619
2. Karimian A, Parsian H, Majidinia M, Rahimi M, Mir SM, Kafil HS, Shafiei-Irannejad V, Kheyrollah M, Ostadi H, Yousefi B (2019) Nanocrystalline cellulose: Preparation, physicochemical properties, and applications in drug delivery systems. Int J Biol Macromol 133:850–859
3. Rajeswari A, Christy EJS, Pius A (2021) Biopolymer blends and composites: processing technologies and their properties for industrial applications. Elsevier, Biopolymers and their industrial applications, pp 105–147
4. Bilal M, Iqbal HM (2019) Naturally-derived biopolymers: Potential platforms for enzyme immobilization. Int J Biol Macromol 130:462–482
5. Hon DN-S (2017) Chemical modification of cellulose. Routledge, Chemical modification of lignocellulosic materials, pp 97–127
6. Brinchi L, Cotana F, Fortunati E, Kenny J (2013) Production of nanocrystalline cellulose from lignocellulosic biomass: technology and applications. Carbohyd Polym 94(1):154–169
7. Fortunati E, Puglia D, Monti M, Peponi L, Santulli C, Kenny J, Torre L (2013) Extraction of cellulose nanocrystals from Phormium tenax fibres. J Polym Environ 21(2):319–328
8. Carels N (2011) The challenge of Bioenergies-an overview. Biofuel's Eng Process Technol 23–64
9. Schubert S, Schlufter K, Heinze T (2011) Configurations, structures, and morphologies of cellulose, Polysaccharides in medicinal and pharmaceutical applications. Shrewsbury iSmithers 1–55
10. Bicu I, Mustata F (2011) Cellulose extraction from orange peel using sulfite digestion reagents. Biores Technol 102(21):10013–10019
11. Shen X-J, Wen J-L, Mei Q-Q, Chen X, Sun D, Yuan T-Q, Sun R-C (2019) Facile fractionation of lignocelluloses by biomass-derived deep eutectic solvent (DES) pretreatment for cellulose enzymatic hydrolysis and lignin valorization. Green Chem 21(2):275–283
12. Shrestha S, Khatiwada JR, Sharma HK, Qin W (2021) Bioconversion of fruits and vegetables wastes into value-added products. Springer, Sustainable Bioconversion of Waste to Value Added Products, pp 145–163
13. Das H, Singh SK (2004) Useful byproducts from cellulosic wastes of agriculture and food industry—a critical appraisal. Crit Rev Food Sci Nutr 44(2):77–89
14. Rajinipriya M, Nagalakshmaiah M, Robert M, Elkoun S (2018) Importance of agricultural and industrial waste in the field of nanocellulose and recent industrial developments of wood based nanocellulose: a review. ACS Sustain Chem Eng 6(3):2807–2828
15. Ramakrishnan A, Ravishankar K, Dhamodharan R (2019) Preparation of nanofibrillated cellulose and nanocrystalline cellulose from surgical cotton and cellulose pulp in hot-glycerol medium. Cellulose 26(5):3127–3141
16. Satlewal A, Agrawal R, Bhagia S, Sangoro J, Ragauskas AJ (2018) Natural deep eutectic solvents for lignocellulosic biomass pretreatment: recent developments, challenges and novel opportunities. Biotechnol Adv 36(8):2032–2050
17. Khan MA, Wahid A, Ahmad M, Tahir MT, Ahmed M, Ahmad S, Hasanuzzaman M (2020) World cotton production and consumption: An overview, Cotton production and uses: Agronomy, crop protection, and postharvest technologies 1–7
18. Ng H-M, Sin LT, Tee T-T, Bee S-T, Hui D, Low C-Y, Rahmat A (2015) Extraction of cellulose nanocrystals from plant sources for application as reinforcing agent in polymers. Compos B Eng 75:176–200
19. Chen H-M, Fu X, Luo Z-G (2015) Properties and extraction of pectin-enriched materials from sugar beet pulp by ultrasonic-assisted treatment combined with subcritical water. Food Chem 168:302–310
20. Kumar B, Bhardwaj N, Agrawal K, Chaturvedi V, Verma P (2020) Current perspective on pretreatment technologies using lignocellulosic biomass: An emerging biorefinery concept. Fuel Process Technol 199:106244
21. Florindo C, Branco LC, Marrucho IM (2019) Quest for green-solvent design: from hydrophilic to hydrophobic (deep) eutectic solvents. Chemsuschem 12(8):1549–1559
22 Torres LAZ, Woiciechowski AL, de AndradeTanobe VO, Karp SG, Lorenci LCG, Faulds C, Soccol CR (2020) Lignin as a potential source of high-added value compounds: A review. J Clean Prod 263:121499
23. H. Soleimanzadeh, F.M. Bektashi, S.Z. Ahari, D. Salari, A. Olad, A. Ostadrahimi (2022) Optimization of cellulose extraction process from sugar beet pulp and preparation of its nanofibers with choline chloride–lactic acid deep eutectic solvents. Biomass Convers Biorefin 1–13
24. Francisco M, Van Den Bruinhorst A, Kroon MC (2012) New natural and renewable low transition temperature mixtures (LTTMs): screening as solvents for lignocellulosic biomass processing. Green Chem 14(8):2153–2157
25. Mallakpour S, Dinari M (2012) Ionic liquids as green solvents: progress and prospects. Green Solvents I I:1–32
26. Halder P, Kundu S, Patel S, Setiawan A, Atkin R, Parthasarthy R, Paz-Ferreiro J, Surapaneni A, Shah K (2019) Progress on the pre-treatment of lignocellulosic biomass employing ionic liquids. Renew Sustain Energy Rev 105:268–292
27. Bhatia SK, Jagtap SS, Bedekar AA, Bhatia RK, Patel AK, Pant D, Banu JR, Rao CV, Kim Y-G, Yang Y-H (2020) Recent developments in pretreatment technologies on lignocellulosic biomass: effect of key parameters, technological improvements, and challenges. Biores Technol 300:122724
28. Usmani Z, Sharma M, Gupta P, Karpichev Y, Gathergood N, Bhat R, Gupta VK (2020) Ionic liquid based pretreatment of lignocellulosic biomass for enhanced bioconversion. Biores Technol 304:123003
29. Mohan M, Goud VV, Banerjee T (2015) Solubility of glucose, xylose, fructose and galactose in ionic liquids: Experimental and theoretical studies using a continuum solvation model. Fluid Phase Equilib 395:33–43
30. Mohan M, Banerjee T, Goud VV (2016) Solid liquid equilibrium of cellobiose, sucrose, and maltose monohydrate in ionic liquids: experimental and quantum chemical insights. J Chem Eng Data 61(9):2923–2932
31. Scott M, Deuss PJ, de Vries JG, Prechtl MH, Barta K (2016) New insights into the catalytic cleavage of the lignin β-O-4

linkage in multifunctional ionic liquid media. Catal Sci Technol 6(6):1882–1891
32. Abbott AP, Boothby D, Capper G, Davies DL, Rasheed RK (2004) Deep eutectic solvents formed between choline chloride and carboxylic acids: versatile alternatives to ionic liquids. J Am Chem Soc 126(29):9142–9147
33. Capolupo L, Faraco V (2016) Green methods of lignocellulose pretreatment for biorefinery development. Appl Microbiol Biotechnol 100(22):9451–9467
34. Pinkert A, Goeke DF, Marsh KN, Pang S (2011) Extracting wood lignin without dissolving or degrading cellulose: investigations on the use of food additive-derived ionic liquids. Green Chem 13(11):3124–3136
35. Hassan SS, Williams GA, Jaiswal AK (2018) Emerging technologies for the pretreatment of lignocellulosic biomass. Biores Technol 262:310–318
36. Hansen BB, Spittle S, Chen B, Poe D, Zhang Y, Klein JM, Horton A, Adhikari L, Zelovich T, Doherty BW (2020) Deep eutectic solvents: A review of fundamentals and applications. Chem Rev 121(3):1232–1285
37. Zhang Q, Vigier KDO, Royer S, Jérôme F (2012) Deep eutectic solvents: syntheses, properties and applications. Chem Soc Rev 41(21):7108–7146
38. Tang X, Zuo M, Li Z, Liu H, Xiong C, Zeng X, Sun Y, Hu L, Liu S, Lei T (2017) Green processing of lignocellulosic biomass and its derivatives in deep eutectic solvents. Chemsuschem 10(13):2696–2706
39. Xu P, Zheng G-W, Zong M-H, Li N, Lou W-Y (2017) Recent progress on deep eutectic solvents in biocatalysis. Bioresources Bioprocessing 4(1):1–18
40. Bystrzanowska M, Tobiszewski M (2021) Assessment and design of greener deep eutectic solvents–A multicriteria decision analysis. J Mol Liq 321:114878
41. Elhamarnah Y, Qiblawey H, Nasser MS, Benamor A (2020) Thermo-rheological characterization of malic acid based natural deep eutectic solvents. Sci Total Environ 708:134848
42. Cicco L, Dilauro G, Perna FM, Vitale P, Capriati V (2021) Advances in deep eutectic solvents and water: applications in metal-and biocatalyzed processes, in the synthesis of APIs, and other biologically active compounds. Org Biomol Chem 19(12):2558–2577
43. Fanali C, Della Posta S, Dugo L, Gentili A, Mondello L, De Gara L (2020) Choline-chloride and betaine-based deep eutectic solvents for green extraction of nutraceutical compounds from spent coffee ground. J Pharma Biomed Anal 189:113421
44. Rashid T, Sher F, Rasheed T, Zafar F, Zhang S, Murugesan T (2021) Evaluation of current and future solvents for selective lignin dissolution–A review. J Mol Liq 321:114577
45. Tan YT, Chua ASM, Ngoh GC (2020) Deep eutectic solvent for lignocellulosic biomass fractionation and the subsequent conversion to bio-based products–A review. Biores Technol 297:122522
46. Bjelić A, Hočevar B, Grilc M, Novak U, Likozar B (2022) A review of sustainable lignocellulose biorefining applying (natural) deep eutectic solvents (DESs) for separations, catalysis and enzymatic biotransformation processes. Rev Chem Eng 38(3):243–272
47. Xu H, Kong Y, Peng J, Song X, Che X, Liu S, Tian W (2020) Multivariate analysis of the process of deep eutectic solvent pretreatment of lignocellulosic biomass. Ind Crops Prod 150:112363
48. Massayev S, Lee KM (2022) Evaluation of deep eutectic solvent pretreatment towards efficacy of enzymatic saccharification using multivariate analysis techniques. J Clean Prod 360:132239
49. Jablonsky M, Haz A, Majova V (2019) Assessing the opportunities for applying deep eutectic solvents for fractionation of beech wood and wheat straw. Cellulose 26:7675–7684
50. Li A-L, Hou X-D, Lin K-P, Zhang X, Fu M-H (2018) Rice straw pretreatment using deep eutectic solvents with different constituents molar ratios: Biomass fractionation, polysaccharides enzymatic digestion and solvent reuse. J Biosci Bioeng 126(3):346–354
51. Álvarez A, Cachero S, González-Sánchez C, Montejo-Bernardo J, Pizarro C, Bueno JL (2018) Novel method for holocellulose analysis of non-woody biomass wastes. Carbohyd Polym 189:250–256
52. Sai YW, Lee KM (2019) Enhanced cellulase accessibility using acid-based deep eutectic solvent in pretreatment of empty fruit bunches. Cellulose 26:9517–9528
53. Maran JP, Manikandan S, Thirugnanasambandham K, Nivetha CV, Dinesh R (2013) Box-Behnken design based statistical modeling for ultrasound-assisted extraction of corn silk polysaccharide. Carbohyd Polym 92(1):604–611
54. Soleimanzadeh H, Niaei A, Salari D, Tarjomannejad A, Penner S, Grünbacher M, Hosseini SA, Mousavi SM (2019) Modeling and optimization of V2O5/TiO2 nanocatalysts for NH3-Selective catalytic reduction (SCR) of NOx by RSM and ANN techniques. J Environ Manage 238:360–367
55. Mali S, Debiagi F, Grossmann MV, Yamashita F (2010) Starch, sugarcane bagasse fibre, and polyvinyl alcohol effects on extruded foam properties: A mixture design approach. Ind Crops Prod 32(3):353–359
56. Panahi PN, Salari D, Niaei A, Mousavi SM (2015) Study of M-ZSM-5 nanocatalysts (M: Cu, Mn, Fe, Co…) for selective catalytic reduction of NO with NH3: Process optimization by Taguchi method. Chin J Chem Eng 23(10):1647–1654
57. Jung S-J, Kim S-H, Chung I-M (2015) Comparison of lignin, cellulose, and hemicellulose contents for biofuels utilization among 4 types of lignocellulosic crops. Biomass Bioenerg 83:322–327
58. Ruiz-Aquino F, González-Peña MM, Valdez-Hernández JI, Revilla US, Romero-Manzanares A (2015) Chemical characterization and fuel properties of wood and bark of two oaks from Oaxaca, Mexico. Ind Crops Prod 65:90–95
59. Thi S, Lee KM (2019) Comparison of deep eutectic solvents (DES) on pretreatment of oil palm empty fruit bunch (OPEFB): Cellulose digestibility, structural and morphology changes. Biores Technol 282:525–529
60. Kumar AK, Shah E, Patel A, Sharma S, Dixit G (2018) Physicochemical characterization and evaluation of neat and aqueous mixtures of choline chloride+ lactic acid for lignocellulosic biomass fractionation, enzymatic hydrolysis and fermentation. J Mol Liq 271:540–549
61. Soares B, da Costa Lopes AM, Silvestre AJ, Pinto PCR, Freire CS, Coutinho JA (2021) Wood delignification with aqueous solutions of deep eutectic solvents. Indus Crops Prod 160:113128
62. Lamaming J, Hashim R, Sulaiman O, Leh CP, Sugimoto T, Nordin NA (2015) Cellulose nanocrystals isolated from oil palm trunk. Carbohyd Polym 127:202–208
63. Johar N, Ahmad I, Dufresne A (2012) Extraction, preparation and characterization of cellulose fibres and nanocrystals from rice husk. Ind Crops Prod 37(1):93–99
64. Oh SY, Yoo DI, Shin Y, Seo G (2005) FTIR analysis of cellulose treated with sodium hydroxide and carbon dioxide. Carbohyd Res 340(3):417–428
65. Hou X-D, Li A-L, Lin K-P, Wang Y-Y, Kuang Z-Y, Cao S-L (2018) Insight into the structure-function relationships of deep eutectic solvents during rice straw pretreatment. Biores Technol 249:261–267
66. Chieng BW, Lee SH, Ibrahim NA, Then YY, Loo YY (2017) Isolation and characterization of cellulose nanocrystals from oil palm mesocarp fiber. Polymers 9(8):355
67. Sun X, Xu F, Sun R, Fowler P, Baird M (2005) Characteristics of degraded cellulose obtained from steam-exploded wheat straw. Carbohyd Res 340(1):97–106

68. Zhao C, Jiang E, Chen A (2017) Volatile production from pyrolysis of cellulose, hemicellulose and lignin. J Energy Inst 90(6):902–913
69. Meda RS, Jain S, Singh S, Verma C, Nandi U, Maji PK (2022) Novel Lagenaria siceraria peel waste based cellulose nanocrystals: Isolation and rationalizing H-bonding interactions. Ind Crops Prod 186:115197
70. Lynam JG, Kumar N, Wong MJ (2017) Deep eutectic solvents' ability to solubilize lignin, cellulose, and hemicellulose; thermal stability; and density. Biores Technol 238:684–689
71. Haafiz MM, Eichhorn S, Hassan A, Jawaid M (2013) Isolation and characterization of microcrystalline cellulose from oil palm biomass residue. Carbohyd Polym 93(2):628–634
72. Wang Z, Yao Z, Zhou J, Zhang Y (2017) Reuse of waste cotton cloth for the extraction of cellulose nanocrystals. Carbohyd Polym 157:945–952
73. Kaushik A, Singh M, Verma G (2010) Green nanocomposites based on thermoplastic starch and steam exploded cellulose nanofibrils from wheat straw. Carbohyd Polym 82(2):337–345
74. Mtibe A, Linganiso LZ, Mathew AP, Oksman K, John MJ, Anandjiwala RD (2015) A comparative study on properties of micro and nanopapers produced from cellulose and cellulose nanofibres. Carbohyd Polym 118:1–8
75 Fareez IM, Ibrahim NA, Wan Yaacob WMH, MamatRazali NA, Jasni AH, Abdul Aziz F (2018) Characteristics of cellulose extracted from Josapine pineapple leaf fibre after alkali treatment followed by extensive bleaching. Cellulose 25(8):4407–4421
76. Gong J, Li J, Xu J, Xiang Z, Mo L (2017) Research on cellulose nanocrystals produced from cellulose sources with various polymorphs. RSC Adv 7(53):33486–33493
77. Sofla MRK, Brown R, Tsuzuki T, Rainey T (2016) A comparison of cellulose nanocrystals and cellulose nanofibres extracted from bagasse using acid and ball milling methods. Adv Nat Sci Nanosci Nanotech 7(3):035004
78. Wang H, Li J, Zeng X, Tang X, Sun Y, Lei T, Lin L (2020) Extraction of cellulose nanocrystals using a recyclable deep eutectic solvent. Cellulose 27:1301–1314
79. Chen W, Yu H, Liu Y, Hai Y, Zhang M, Chen P (2011) Isolation and characterization of cellulose nanofibers from four plant cellulose fibers using a chemical-ultrasonic process. Cellulose 18(2):433–442
80. Martins MA, Teixeira EM, Corrêa AC, Ferreira M, Mattoso LH (2011) Extraction and characterization of cellulose whiskers from commercial cotton fibers. J Mater Sci 46(24):7858–7864
81. Shen D, Gu S, Bridgwater A (2010) The thermal performance of the polysaccharides extracted from hardwood: Cellulose and hemicellulose. Carbohyd Polym 82(1):39–45
82. Xie J, Hse C-Y, Cornelis F, Hu T, Qi J, Shupe TF (2016) Isolation and characterization of cellulose nanofibers from bamboo using microwave liquefaction combined with chemical treatment and ultrasonication. Carbohyd Polym 151:725–734
83. Zhao J, Zhang W, Zhang X, Zhang X, Lu C, Deng Y (2013) Extraction of cellulose nanofibrils from dry softwood pulp using high shear homogenization. Carbohyd Polym 97(2):695–702
84. Ferreira F, Mariano M, Rabelo S, Gouveia R, Lona L (2018) Isolation and surface modification of cellulose nanocrystals from sugarcane bagasse waste: from a micro-to a nano-scale view. Appl Surf Sci 436:1113–1122
85. Chundawat SP, Donohoe BS, da Costa Sousa L, Elder T, Agarwal UP, Lu F, Ralph J, Himmel ME, Balan V, Dale BE (2011) Multi-scale visualization and characterization of lignocellulosic plant cell wall deconstruction during thermochemical pretreatment Energ. Environ Sci 4(3):973–984